Alexandria Engineering Journal (2014) 53, 355–371

FACULTY OF ENGINEERING ALEXANDRIA UNIVERSITY

Alexandria University

Alexandria Engineering Journal

www.elsevier.com/locate/aej
www.sciencedirect.com

ORIGINAL ARTICLE

Bond behavior and assessment of design ultimate bond stress of normal and high strength concrete

Ahmed M. Diab, Hafez E. Elyamany *, Mostafa A. Hussein, Hazem M. Al Ashy

Structural Engineering Department, Alexandria University, Egypt

Received 11 January 2014; revised 15 March 2014; accepted 27 March 2014
Available online 29 April 2014

KEYWORDS

Bond strength;
Single and double pull-out test;
High strength concrete;
Design ultimate stress

Abstract The aim of this work is to assess the ultimate bond stress of normal and high strength concrete. This study contains two phases. The first phase included the studied bond behavior using two different models. In the first model, single pull-out test (SPOT), the concrete section of specimen was subjected to compressive stresses. In the second model, double pull-out test (DPOT), the concrete section of specimen was subjected to tensile stresses. So this phase of study aimed to make a comparison between the single pull-out test and the double pull-out test. To compare the behavior of these models, different levels of compressive strength were considered through the use of different coarse aggregate types, different W/C ratios and different cement contents. The second phase focused on the study of bond strength of high strength concrete using double pull-out test to assess design ultimate bond stress. In this phase, the effect of concrete compressive strength, bar diameter, concrete cover, embedded length, and pre-flexural crack length was studied. Based on the test results, a proposed concept to assess design ultimate stress of normal and high strength concrete was adopted. Equations to calculate the design ultimate bond stress, and required development length were suggested.

1. Introduction

Bond refers to the interaction between reinforcing steel and the surrounding concrete, which allows transferring of tensile stress from the steel into the concrete. It is the mechanism that allows the anchorage of straight reinforcing bars and influences many other important features of structural concrete such as crack control and section stiffness [1]. Similarly the bond between concrete and development length of reinforcing steel is essential for composite action in reinforced concrete construction [2,3]. It is well known that the use of deformed bars can greatly enhance the steel–concrete bond capacity. Three main components determine the bond strength between the adjacent ribs of a reinforcement bar. These components are shear stresses due to adhesion along the bar surface, the bearing stresses against the faces of ribs (mechanical interlock), and the friction between bars with concrete in the rib dales and

* Corresponding author. Tel.: +20 1099277173.
E-mail address: h_elyamany@yahoo.com (H.E. Elyamany).
Peer review under responsibility of Faculty of Engineering, Alexandria University.

ELSEVIER Production and hosting by Elsevier

1110-0168 © 2014 Production and hosting by Elsevier B.V. on behalf of Faculty of Engineering, Alexandria University.
http://dx.doi.org/10.1016/j.aej.2014.03.012

the surrounding concrete. The highest contribution to bond strength comes from mechanical interlock [4].

Adequate bonding between reinforcing bars and concrete is essential for the satisfactory performance of reinforced concrete structures. In the absence of sufficient bond strength, effective beam action, as required by codes of practice, cannot be achieved, and hence, the specified design equations are no longer valid. Loss of strain compatibility at the depth of a reinforcement results in a redistribution of stresses in the reinforced concrete element, which may lead to excessive service deflections and altered load capacities [5]. One way to evaluate the steel–concrete bond is to investigate the bond stress–slip evolution generally obtained through classical pull-out tests [6]. Even if these tests are not totally satisfactory due to boundary conditions or stress state [7] and replaced by other experimental setups (direct tension-pullout bond test [7]), they remain the most convenient and simplest experiment to achieve a global estimation of the bond effect. The main characteristics of the bond stress–slip evolution and especially the maximum bond stress are found to be clearly dependent on material, geometrical or loading parameters. The positive effect of the spacing and height of ribs was investigated by Hamad [8] and Castel et al. [9]. The confinement was defined as one of the key parameters which influenced the value of the maximum bond stress. This point is of great concern especially in the case of structures which are reinforced with stirrups or submitted to a tri-axial state of stress [10,11]. Torre-Casanova et al. showed [12] that the splitting and pull-out failures depend on the concrete cover (splitting failure for low concrete covers and pull-out failure for others cases).

Also some factors affect negatively the bond strength such as epoxy coating. This effect is due to reduction in adhesion and frictional components along the smooth epoxy surface [13]. Compared with uncoated bars, the decrease in bond strength was found to range from 15% to 50% depending on several factors such as the coating thickness, bar size and location, deformation patterns, concrete properties, and casting conditions [14–16]. Therefore, to compensate such loss, design codes stipulated an increase in the development length of the bars. For example, in ACI 318, the development length is multiplied by a factor of 1.5 for epoxy-coated bars with a cover of less than 3 d_b or clear spacing between bars less than 6 d_b (where d_b is the bar diameter), and a factor of 1.2 for other cases [17]. In the AASHTO bridge specification, these factors are 1.5 and 1.15, respectively [18].

The bond strength of high strength concrete is improved significantly. Many researches have been conducted to give the best expression of the bond strength of this type of concrete. Zsutty [19] found that $\acute{f}_c^{1/3}$ provided an improved match with data compared to $\acute{f}_c^{1/2}$. Darwin et al. [20] combined their own test results with large international database and observed that a best fit with existing data was obtained using $\acute{f}_c^{1/4}$ to represent the effect of compressive strength on development and splice length. Zuo and Darwin [21] also observed that $\acute{f}_c^{1/4}$ provides the best representation for the effect of compressive strength contribution to bond strength. For bar confined by transverse reinforcement, Zuo and Darwin [21] found that $\acute{f}_c^{1/2}$ significantly under-estimates the effect of concrete strength on the additional bond strength provided by transverse reinforcement.

The aim of this study is to make a comparison between the single pull-out test and the doubled pull-out test. Also proposed equations are constructed to assess the design ultimate stress of normal and high strength concrete.

2. Experimental program

2.1. Materials

The experimental program includes two phases. In the first phase (I), three types of coarse aggregate, 19 mm crushed pink limestone, 12 mm gravel and 19 mm crushed dolomite with specific gravity of 2.48, 2.65 and 2.70, respectively were used. Natural siliceous sand with fineness modulus of 2.57 and specific gravity of 2.63 was used. The used aggregates meet ASTM C33 requirements. Silica fume of 10% cement replacement meeting the requirements of ASTM C 1240 was used in some mixes of dolomite concrete. Different cement contents, water cement ratios and type F high range water reducing with different doses presented in Table 1 were considered in this phase.

In the second phase (II) the previous crushed dolomite, natural siliceous sand of 2.6 specific gravity and 2.4 fineness modulus, Silica fume and type F high range water reducing were used. The used dosage of the admixtures was determined by trial to achieve a constant slump of 100 ± 20 mm. Table 2 shows the concrete mixtures of phase II. Portland cement type I according to ASTM C150 was used in this study. In phase I, one deformed steel bar with diameter of 16 mm was used while two different deformed bars of 16 mm, and 18 mm diameter were used in phase II. The properties of the used steel bars are shown in Table 3.

2.2. Test specimen

In the first phase two different configuration test specimens were used. The first was a cube specimen of 150 × 150 × 150 mm with a steel bar of ∅16 mm in the middle as shown in Fig. 1, where the concrete in this specimen was subjected to compressive stress. The second one was prismatic specimens of 150 × 150 × 320 mm in dimension containing two bars of ∅16 mm which were put exactly in the same level and in the opposite direction with 2 cm space between each other, each bar was fixed to a steel chair of ∅8 mm, and the detail of this specimen is shown in Fig. 2. The cross section of specimen was reinforced with four bars of 12 mm and two stirrups were put at the end of the specimen. During the test, the two opposite bars were subjected to a tensile force that which is transferred to the concrete as tensile stresses throughout the bond stresses between the concrete and the steel. The used cover and embedded length of this specimen were 67 mm and 160 mm, respectively. Each result for different tests represents the average of two specimens.

In the second phase, prismatic specimens of 100 × 100 × 325 mm, 150 × 150 × 325 mm, and 150 × 150 × 365 mm were used as shown in Fig. 2. The specimens in phases I and II were cured in water for 28 days until test date. In phase II, the bar slip was recorded for each applied load until failure.

The bond strength was computed using the following equation:

$$\tau = P/(\pi L_m d_b) \quad (1)$$

where τ is the bond strength, P is the ultimate load, L_m is the embedded length, and d_b is the bar diameter.

Table 1 Pink lime stone and gravel concrete mixes in phase I and pull-out bond strength test results.

Type of coarse agg.	Mix no.	W/C	Cement content (kg/m^3)	Admi. (L/m^3)	Slump (cm)	7-Days test results: Ultimate pull-out bond strength (MPa) SPBS (τ_s)	7-Days: Ultimate pull-out bond strength (MPa) DPBS (τ_u)	7-Days: Cube comp. strength (f_{cu}) (MPa)	28-Days test results: Ultimate pull-out bond strength (MPa) SPBS (τ_s)	28-Days: Ultimate pull-out bond strength (MPa) DPBS (τ_u)	28-Days: Cube comp. strength (f_{cu}) (MPa)
Pink lime stone	L01	0.65	250	3.75	20	5.24	4.24	18.7	6.30	5.36	24.4
	L02	0.63	250	3.75	18	5.68	4.64	18.9	6.76	5.90	23.6
	L03	0.60	300	4.50	17	5.83	5.14	19.0	7.02	6.32	25.2
	L04	0.58	300	4.50	15	6.47	5.33	20.0	7.62	6.69	28.8
	L05	0.55	350	5.25	14	6.72	5.77	20.0	7.96	7.02	30.0
	L06	0.45	375	5.63	12	7.07	6.17	26.0	8.40	7.37	38.0
	L07	0.4	400	6.00	10	7.36	6.64	30.0	9.02	7.67	42.0
	L08	0.38	425	6.38	8	7.69	6.63	32.3	9.34	7.96	50.0
	L09	0.35	450	6.75	7	8.02	7.02	35.1	9.87	8.28	55.0
	L10	0.33	475	7.13	6	8.42	7.35	37.8	10.30	8.75	57.0
	L11	0.30	500	7.50	5	8.40	7.82	39.9	10.60	9.12	60.0
Gravel	G01	0.65	250	3.00	22	3.14	2.97	14.9	5.00	4.68	18.0
	G02	0.625	250	3.20	20	3.56	3.34	18.0	5.30	4.99	22.6
	G03	0.6	300	3.70	18	4.03	3.11	18.1	5.66	5.21	23.4
	G04	0.575	300	3.85	17	4.61	3.87	17.9	6.28	5.45	23.9
	G05	0.55	350	4.00	15	5.45	4.12	18.7	6.47	5.71	24.9
	G06	0.45	375	4.20	12	5.66	4.58	22.5	6.74	6.16	28.0
	G07	0.4	400	4.50	10	6.26	5.00	27.0	7.18	6.46	31.1
	G08	0.375	425	4.80	9	6.30	5.40	30.0	7.59	7.02	32.2
	G09	0.35	450	4.95	8	6.69	5.85	32.1	7.97	7.43	33.7
	G10	0.325	475	5.05	8	7.11	6.28	34.6	8.31	7.72	35.8
	G11	0.3	500	5.15	7	7.43	6.50	36.7	9.02	7.97	38.0

Type of coarse agg.	Mix no.	W/C_m	Cement content (kg/m^3)	Silica fume (kg/m^3)	Admixture (L/m^3)	Slump (cm)	7-Days test results: Ultimate pull-out bond strength (MPa) SPBS (τ_s)	7-Days: Ultimate pull-out bond strength (MPa) DPBS (τ_u)	7-Days: Cube comp. strength (f_{cu}) (MPa)	28-Days test results: Ultimate pull-out bond strength (MPa) SPBS (τ_s)	28-Days: Ultimate pull-out bond strength (MPa) DPBS (τ_u)	28-Days: Cube comp. strength (f_{cu}) (MPa)
Dolomite concrete mixes in phase I and pull-out bond strength test results												
Dolomite	D01	0.35	450	0.0	6.70	9.0	6.68	6.03	40.0	9.55	8.62	50.6
	D02	0.30	500	0.0	7.50	7.0	7.17	6.50	44.0	10.25	9.28	53.7
	D03	0.325	475	0.0	7.15	8.0	7.61	6.68	45.0	10.87	9.55	60.5
	D04	0.269	450	50.0	9.30	6.5	7.72	6.96	47.0	11.03	9.95	67.1
	D05	0.25	405	45.0	11.0	6.5	9.06	7.43	53.7	12.94	10.61	76.8
	D06	0.227	450	50.0	9.60	6.5	9.58	8.17	57.8	13.68	11.67	82.5
	D07	0.24	495	55.0	9.20	5.5	9.80	8.35	59.3	14.00	11.93	84.7
	D08	0.224	517.5	57.5	9.00	5.0	10.32	8.88	60.7	14.75	12.69	86.7
	D09	0.227	540	60.0	8.90	6.0	10.80	9.47	61.6	15.43	13.53	88.0
	D10	0.222	562.5	62.5	8.76	4.0	11.06	10.02	67.8	15.81	14.32	96.8

Table 2 Concrete mixes in phase II.

Mix no.	W/C_m	Cement content (kg/m^3)	Silica fume (kg/m^3)	Admixture (L/m^3)	Slump (cm)	28-Days achieved compressive strength (MPa)	28-Days target compressive strength (MPa)
1	0.56	350	0.00	3.00	10.0	33.0	30
2	0.40	450	0.00	5.50	9.50	48.9	50
3	0.26	600	60.0	13.5	10.5	72.0	70
4	0.24	600	60.0	14.5	10.0	88.2	90

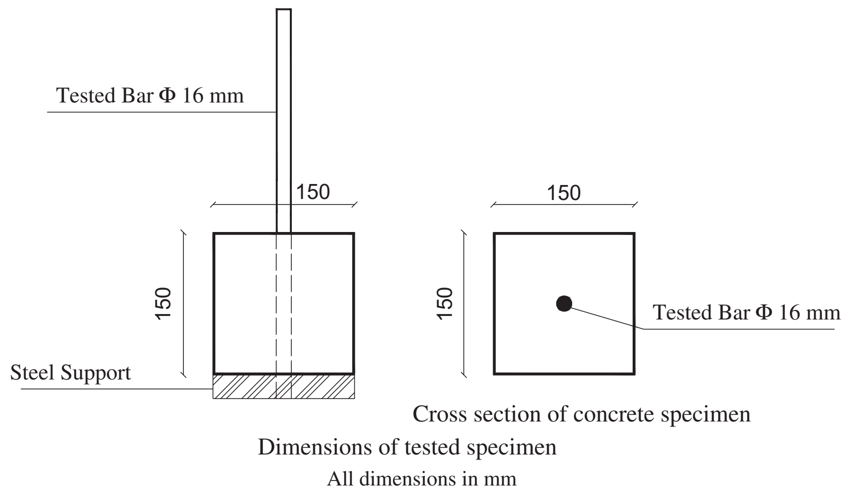

Figure 1 Single pull-out specimen.

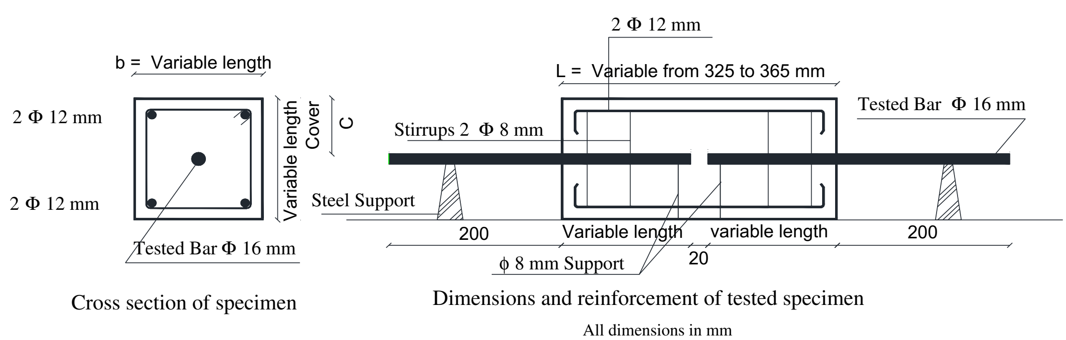

Figure 2 Tensile pull-out (double) bond specimen.

Table 3 Properties of used steel bars.

Phase	Diameter (mm)	Core diameter (mm)	Rib height (h_r) (mm)	Rib spacing (s_r) (mm)	Yield strength (MPa)	Ultimate strength (MPa)	Elongation (%)
I	16	14.92	1.34	11.2	410	560	18.5
II	16	15.00	1.00	20.83	360	520	25.0
	18	17.20	1.10	20.83	360	520	24.0

2.3. Test variables

The variables studied throughout the first phase of this study were types of coarse aggregate (crushed pink lime stone, gravel and crushed dolomite) and cube compressive strength by changing cement content and water cement ratio as presented in Table 1, while the variables in the second phase were cube compressive strength of 30, 50, 70, and 90 MPa, concrete cover (C) of 67, and 42 mm, bar diameter of 16, and 18 mm, embedded length of 5 d_b, 7.5 d_b, and 10

Table 4 Specimen dimensions, and test variables of phase II.

Specimen no.	L (mm)	b (mm)	C (mm)	d_b (mm)	L_m (mm)	Ultimate tensile pull-out bond strength (τ_u) (MPa)	Ultimate slip (mm)	f_{cu} (MPa)	Presence of cracks
1	325	150	67	16	160	5.67	1.05	30	Un-cracked
2	325	150	67	16	160	6.85	0.523	50	Un-cracked
3	325	150	67	16	160	7.97	0.46	70	Un-cracked
4	325	150	67	16	160	10.45	0.377	90	Un-cracked
5	325	150	67	16	160	6.97	0.60	50	Un-cracked
6	325	150	67	16	160	8.20	0.587	70	Un-cracked
7	325	100	42	16	160	5.47	1.40	30	Un-cracked
8	325	100	42	16	160	6.37	0.86	50	Un-cracked
9	325	100	42	16	160	6.97	0.80	70	Un-cracked
10	325	100	42	16	160	8.46	0.55	90	Un-cracked
11	365	150	66	18	180	5.10	1.53	30	Un-cracked
12	365	150	66	18	180	6.45	1.12	50	Un-cracked
13	365	150	66	18	180	7.46	0.78	70	Un-cracked
14	365	150	66	18	180	9.95	0.74	90	Un-cracked
15	325	150	67	16	160	6.85	0.523	50	Un-cracked
16	325	150	67	16	120	6.494	0.43	50	Un-cracked
17	325	150	67	16	80	6.22	0.35	50	Un-cracked
18	325	150	67	16	160	6.28	0.58	50	[a]Cracked
19	325	150	67	16	160	5.60	0.78	50	[b]Cracked
20	325	150	67	16	160	5.04	0.94	50	[c]Cracked

[a] Length of cracks is 75 mm (half cracked specimen).
[b] Length of cracks is 125 mm (three-quarter cracked specimen).
[c] Length of cracks is 150 mm (fully cracked specimen).

d_b and pre-flexural crack length of 75, 125, and 150 mm. Three specimens were pre-loaded in flexure to obtain a different crack length, and after flexural cracking, these specimens were tested in tensile pull-out bond test. Table 4 shows tested specimens and variables in the second phase.

3. Results and discussions

3.1. Relation between single pull-out and double pull-out bond strength at different values of compressive strength

Fig. 3 shows the relation between cube compressive strength and both single and double pull-out bond strength for concrete made of different types of coarse aggregate for phase I. From this figure, as the compressive strength increases, both single and double pull-out bond strength increase. As an example, the single and double pull-out bond strength for lime stone increases by 27.8% and 25.3% as the compressive strength increases from 30 to 50 MPa. So, compressive strength of concrete has a significant effect on bond strength. This is in an agreement with Zuo and Darwin [21] and Hadi [22]. The enhancement of compressive strength improves bearing, cohesion and friction strength.

The double pull-out bond strength (tensile pull-out bond strength) is lower than the single pull-out bond strength at the same compressive strength. Also, at the same compressive strength, both single and double pull-out strength depend upon the type of coarse aggregate, where the used crushed aggregate has higher values of pull-out bond strength compared with that of gravel. Moreover, the crushed dolomite gives the highest values of pull-out bond strength.

From Table 1 and Fig. 3, the ratio between double pull-out bond strength and single pull-out bond strength (Ri) was calculated using test results for different types of coarse aggregate. The average ratio ($\overline{Ru}$), standard deviation $\delta n-1$ and characteristic ratio Ru_1 and Ru_2 at probability of 5.5% and 1.1% are presented in Table 4. From the results presented in Table 5, the average value of percentage of tensile pull-out bond to single pull-out bond strength for concrete made of lime stone or dolomite is almost the same (≈87%) while this percentage of gravel concrete is 91.2%. It is recommended to use the single pull-out bond test to calculate the tensile pull-out bond strength (τ_u) because it is easy to carry out this test. The characteristic tensile pull-out bond strength ($\overline{\tau}_u$)) can be calculated using single pull-out test as follows;

$$\overline{\tau}_u = R_u \tau_s \tag{2}$$

where $Ru = 0.822$, 0.856 and 0.809 for limestone, gravel and dolomite concrete at a probability of 1.1% respectively.

3.2. Bond stress–slip relationship

In phase II, Figs. 4–8 show the bond stress–slip relationship for specimens of $150 \times 150 \times 325$, $100 \times 100 \times 325$, and $150 \times 150 \times 365$ mm. From these figures, it is shown that as the bond stress increases the slip increases in almost a constant rate till a certain point after which the slope of the curve changes until it reaches the ultimate strength then the curve goes down. Furthermore, it is obvious that concretes of 70 and 90 MPa cube compressive strength failed in a brittle manner, and the specimens failed abruptly forming longitudinal splitting cracks as shown in Fig. 9, moreover the bond stress reduces drastically as shown. This can be explained on the basis of fracture mechanism.

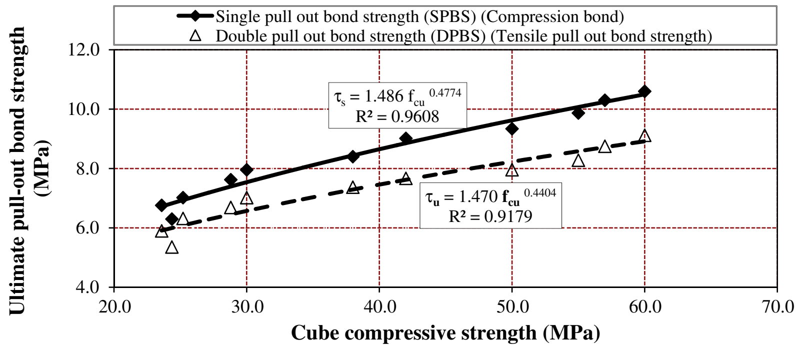

(a) Lime stone concrete

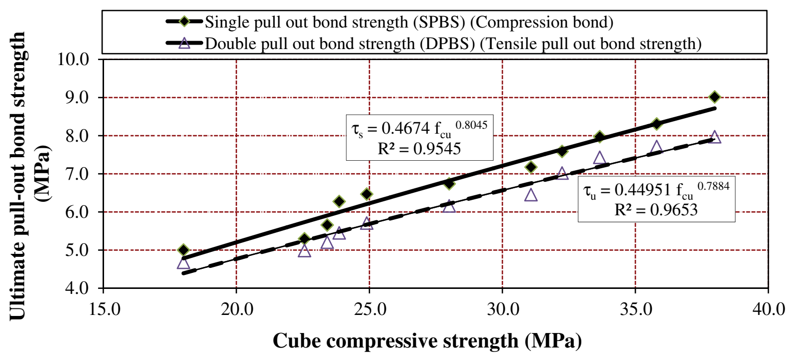

(b) Gravel concrete

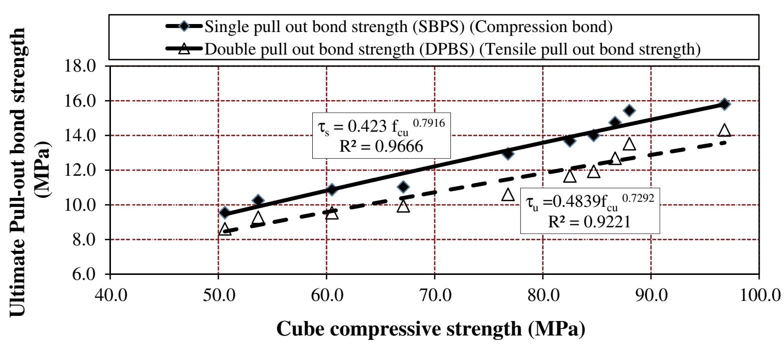

(c) Dolomite concrete

Figure 3 Effect of 28-days cube compressive strength on both single and double pull-out strength for lime stone, gravel and dolomite concrete.

Table 5 Average value of percentage of tensile pull-out bond to single pull-out bond strength.

Type of coarse aggregate	Average (%) $\overline{Ru}$)	$\sigma_{n-1\%}$	$Ru_{1\%}$	$Ru_2\%$
Lime stone	86.5	1.86	83.5	82.2
Gravel	91.2	2.45	87.3	85.6
Dolomite	87.6	2.92	82.9	80.9

According to energy criterion of fracture mechanism, strain energy keeps on accumulating in the material as microcracking propagates at about 70–80% of the ultimate. As soon as a primary crack forms along the boundary between steel and concrete, it immediately leads to crack propagation utilizing accumulating energy. Formation of longitudinal splitting cracks occurs rapidly causing the bond failure in highly abrupt and brittle manner [23].

3.3. Effect of concrete cover

Fig. 10 shows the effect of the concrete cover on ultimate tensile bond strength and ultimate slip. It is obvious that as the concrete cover decreases, the ultimate bond strength decreases, and the corresponding slip increases. As an example, when the concrete cover decreases from 67 to 42 mm the ultimate bond strength decreases by 4%, 8%, 12.5% and

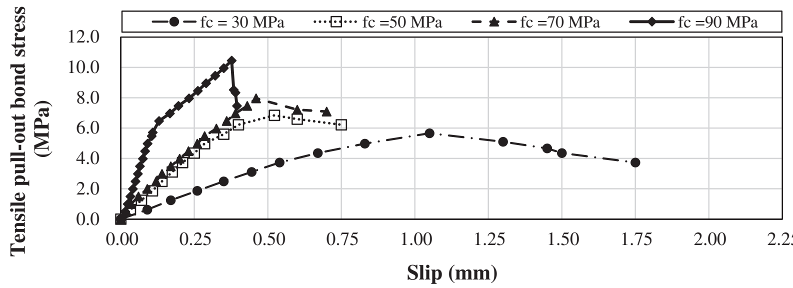

Figure 4 Bond stress–slip relationship for $150 \times 150 \times 325$ specimens with 16 mm bar diameter and 160 mm development length for different compressive strengths.

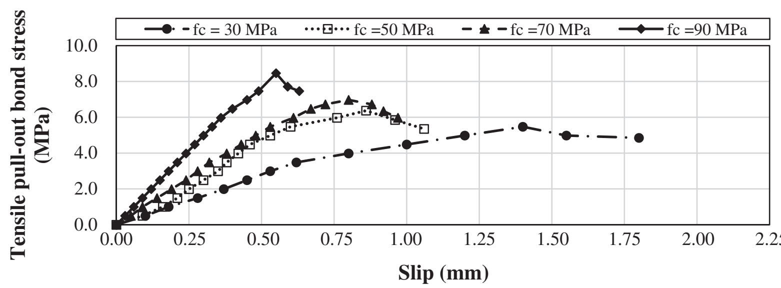

Figure 5 Bond stress–slip relationships for $100 \times 100 \times 325$ specimens with 16 mm bar diameter and 160 mm development length for different compressive strengths.

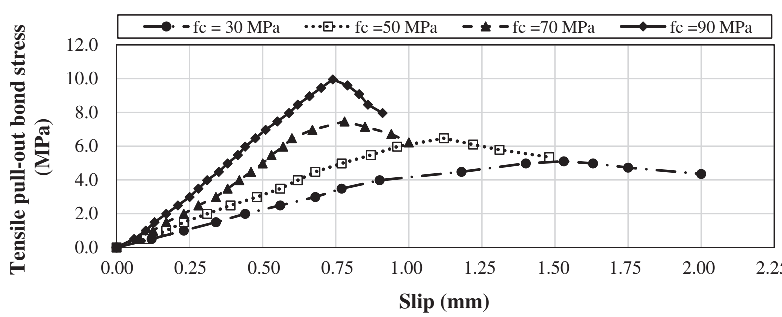

Figure 6 Bond stress–slip relationships for $150 \times 150 \times 365$ specimens with 18 mm bar diameter and 180 mm development length for different concrete compressive strengths.

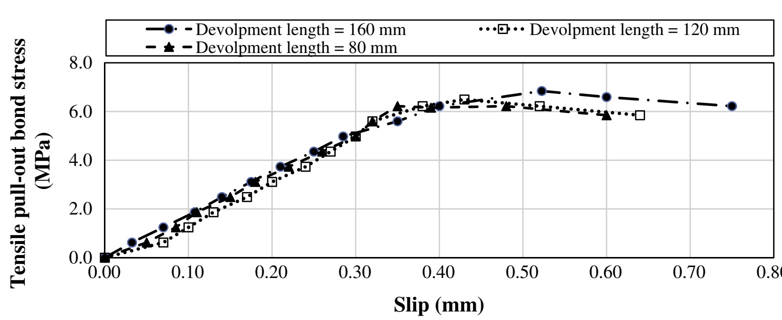

Figure 7 Bond stress–slip relationships for $150 \times 150 \times 365$ specimens with 16 mm bar diameter and different development lengths for concrete compressive strength of 50 MPa.

19% for compressive strength of 30, 50, 70 and 90 MPa, respectively. This is in an agreement with Darwin et al. [20], and Zuo and Darwin [21]. This can be explained on the basis of the increase in confinement that offers more resistance to longitudinal cracks and reduces the uneven bond stress distribution along the embedded lengths [12]. High strength concrete may require higher concrete cover.

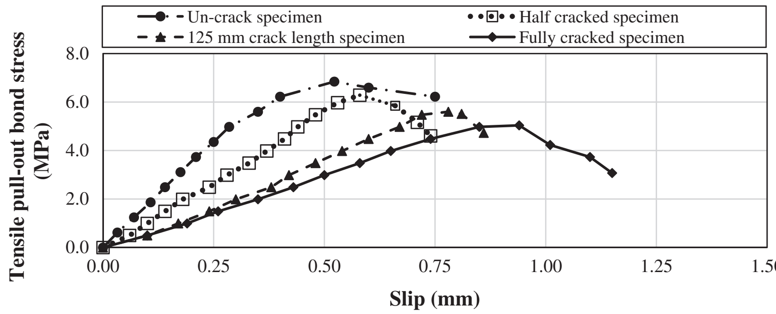

Figure 8 Bond stress–slip relationships for 150 × 150 × 365 specimens with 16 mm bar diameter, 160 mm development length and different crack lengths for concrete compressive strength of 50 MPa.

(a) f_{cu} = 30 MPa (b) f_{cu} = 50 MPa (c) f_{cu} = 70 MPa (d) f_{cu} = 90 MPa

Figure 9 Failure cracks for 150 × 150 × 325 mm specimen with different compressive strength, 16 mm bar diameter, and 160 mm development length.

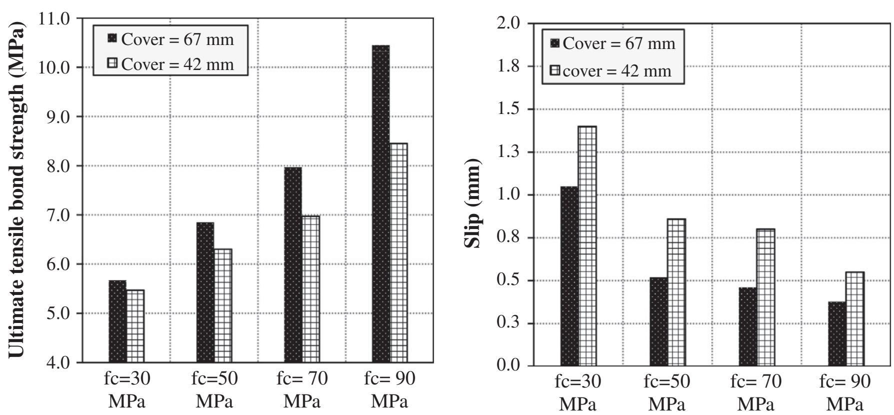

Figure 10 Effect of concrete cover on ultimate tensile bond strength and ultimate slip for specimens of 150 × 150 × 325 and 100 × 100 × 325 mm.

3.4. Effect of bar diameter

Fig. 11 shows the effect of bar diameter on ultimate tensile bond strength and ultimate slip. It is shown that as the bar diameter increases, the bond strength decreases, and the corresponding slip increases. As an example, the ultimate tensile bond strength decreases by 10%, 6%, 6% and 5% when the bar diameter increases from 16 to 18 mm for concrete compressive strength 30, 50, 70 and 90 MPa, respectively. This is in an agreement with Kazim Turk [23] and Alavi-Fard and Marzouk [24].

3.5. Effect of embedded length

Fig. 12 shows the effect of embedded length on both ultimate tensile bond strength, and ultimate slip. It is shown that as the used embedded length increases, the ultimate bond strength increases, and the corresponding slip increases. When the development length increases from 5 bar diameter to 7.5 and 10 bar diameter the bond strength increases by 4.3% and 10.0%, respectively. This is in an agreement with Ahmed et al. [25].

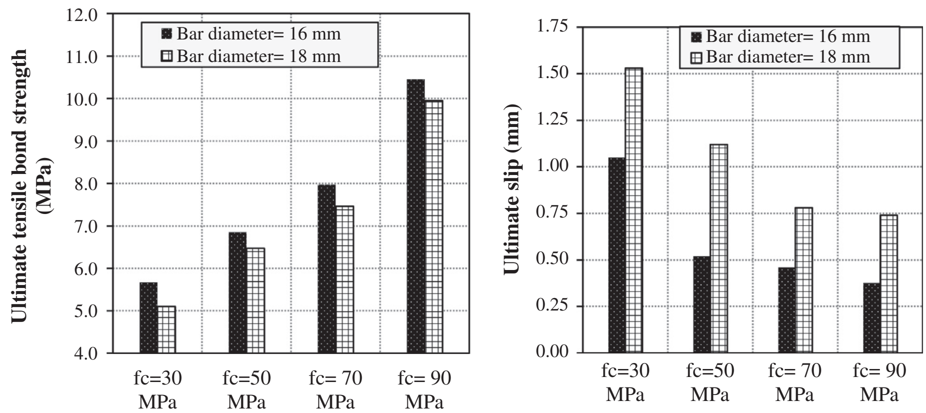

Figure 11 Effect of bar diameter on ultimate tensile bond strength and ultimate slip for specimens of 150 × 150 × 325 with 16 mm bar diameter and 150 × 150 × 365 with 18 mm bar diameter.

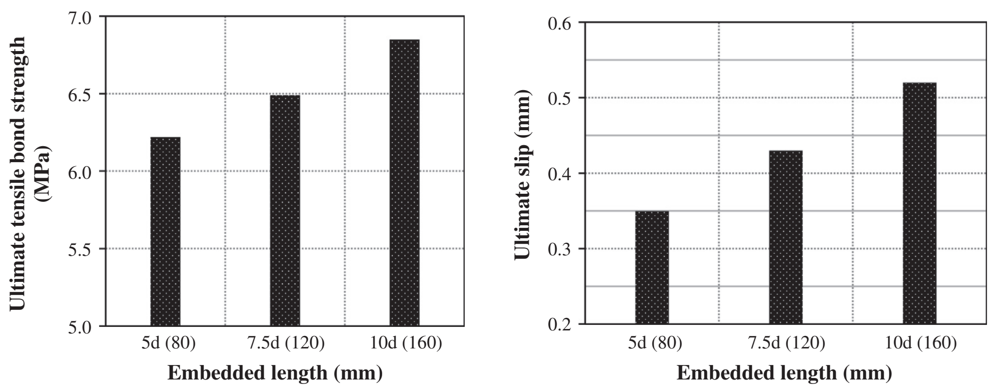

Figure 12 Effect of embedded length on ultimate tensile bond strength and ultimate slip for specimen of 150 × 150 × 325 mm with 16 mm bar diameter, and 50 MPa cube compressive strength.

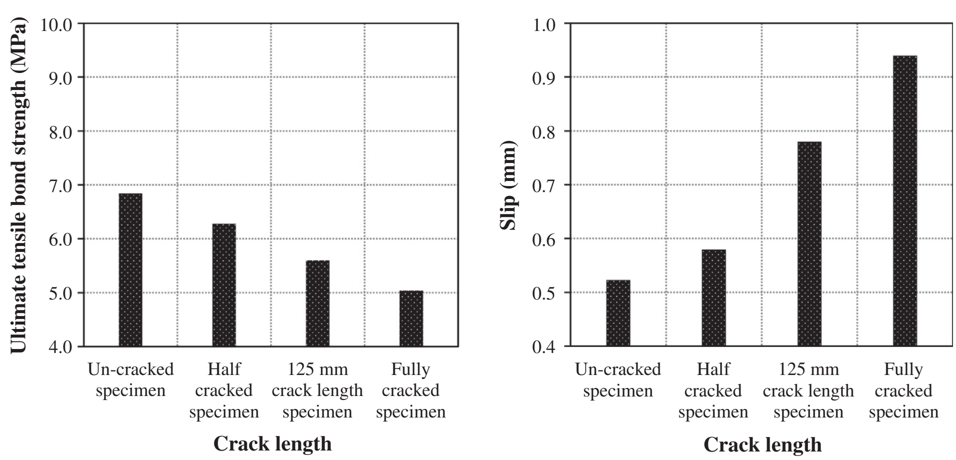

Figure 13 Effect of crack length on ultimate tensile bond strengths and ultimate slip for specimen of 150 × 150 × 325 mm with 16 mm bar diameter, and 50 MPa cube compressive strength.

3.6. Effect of pre-flexural crack length

Fig. 13 shows the effect of crack length on both ultimate tensile bond strength, and ultimate slip. It is shown that as the crack length increases the ultimate tensile bond strength decreases, and the corresponding slip increases. The fully cracked specimen loses about 30% of its bond strength. The presence of cracks decreases the stiffness of concrete section, and makes the distribution of the bond stress non-uniform along the bar. This result may be due

Table 6 Comparison of ultimate bond strength calculated from different equations and the experimental bond strength for pink lime stone and gravel concrete (d_b = 16 mm, C = 67 mm, L_m = 160 mm, h_r = 2.68 mm and s_r = 11.2 mm).

Type of coarse agg.	Mix no.	Ultimate bond strength (MPa)							Experimental test result/prediction ratios for bond strength					
		Experiment (a)	Orangun et al. (1)	Drawin et al. (2)	Muhammad Hadi (3)	Esfahani and Rangan (4)	ACI Committee 408 (5)	Proposed Eq. (6)	(a)/(1)	(a)/(2)	(a)/(3)	(a)/(4)	(a)/(5)	(a)/(6)
Pink lime stone	L01	5.36	6.88	6.13	6.64	5.56	7.50	5.80	0.78	0.87	0.81	0.96	0.71	0.92
	L02	5.90	6.77	6.03	6.53	5.47	7.44	5.71	0.87	0.98	0.90	1.08	0.79	1.03
	L03	6.32	7.00	6.24	6.75	5.65	7.56	5.90	0.90	1.01	0.94	1.12	0.84	1.07
	L04	6.69	7.48	6.67	7.22	6.04	7.82	6.31	0.89	1.00	0.93	1.11	0.86	1.06
	L05	7.02	7.63	6.80	7.37	6.17	7.90	6.44	0.92	1.03	0.95	1.14	0.89	1.09
	L06	7.37	8.59	7.66	8.29	6.94	8.38	7.25	0.86	0.96	0.89	1.06	0.88	1.02
	L07	7.67	9.03	8.05	8.72	7.30	8.59	7.62	0.85	0.95	0.88	1.05	0.89	1.01
	L08	7.96	9.85	8.78	9.51	7.96	8.97	8.31	0.81	0.91	0.84	1.00	0.89	0.96
	L09	8.28	10.34	9.21	9.97	8.35	9.19	8.72	0.80	0.90	0.83	0.99	0.90	0.95
	L10	8.75	10.52	9.38	10.15	8.50	9.27	8.87	0.83	0.93	0.86	1.03	0.94	0.99
	L11	9.12	10.80	9.62	10.42	8.72	9.39	9.10	0.84	0.95	0.88	1.05	0.97	1.00
	Mean values								0.85	0.95	0.88	1.05	0.87	1.01
	Standard deviation								0.04	0.05	0.05	0.06	0.07	0.05
Gravel	G01	4.68	5.91	5.27	5.71	4.78	6.95	4.99	0.79	0.89	0.82	0.98	0.67	0.94
	G02	4.99	6.62	5.90	6.39	5.35	7.36	5.58	0.75	0.85	0.78	0.93	0.68	0.89
	G03	5.21	6.74	6.01	6.51	5.45	7.42	5.69	0.77	0.87	0.80	0.96	0.70	0.92
	G04	5.45	6.81	6.07	6.57	5.50	7.46	5.74	0.80	0.90	0.83	0.99	0.73	0.95
	G05	5.71	6.95	6.20	6.71	5.62	7.54	5.87	0.82	0.92	0.85	1.02	0.76	0.97
	G06	6.16	7.37	6.57	7.12	5.96	7.76	6.22	0.84	0.94	0.87	1.03	0.79	0.99
	G07	6.46	7.77	6.92	7.50	6.28	7.97	6.55	0.83	0.93	0.86	1.03	0.81	0.99
	G08	7.02	7.91	7.05	7.64	6.39	8.04	6.67	0.89	1.00	0.92	1.10	0.87	1.05
	G09	7.43	8.09	7.21	7.80	6.53	8.13	6.82	0.92	1.03	0.95	1.14	0.91	1.09
	G10	7.72	8.34	7.43	8.05	6.74	8.26	7.03	0.93	1.04	0.96	1.15	0.93	1.10
	G11	7.97	8.59	7.65	8.29	6.94	8.38	7.24	0.93	1.04	0.96	1.15	0.95	1.10
	Mean values								0.84	0.95	0.87	1.04	0.80	1.00
	Standard deviation								0.06	0.07	0.07	0.08	0.10	0.07

Table 7 Comparison of ultimate bond strength calculated from different equations and the experimental bond strength for dolomite concrete.

Sp. no.	Dimensions (mm)					Ultimate bond strength (MPa)							Experimental test result/prediction ratios for bond strength					
	c	d_b	L_m	h_r	s_r	Experiment (a)	Orangun et al. (1)	Drawin et al. (2)	Muh.mad Hadi (3)	Esfahani and Rangan (4)	ACI Committee 408 (5)	Proposed Eq. (6)	(a)/(1)	(a)/(2)	(a)/(3)	(a)/(4)	(a)/(5)	(a)/(6)
D01	67	16	160	1.34	11.2	8.62	9.91	8.84	9.57	8.01	9.00	8.36	0.87	0.98	0.90	1.08	0.96	1.03
D02	67	16	160	1.34	11.2	9.28	10.21	9.10	9.85	8.25	9.14	8.61	0.91	1.02	0.94	1.13	1.02	1.08
D03	67	16	160	1.34	11.2	9.55	10.84	9.66	10.46	8.76	9.41	9.14	0.88	0.99	0.91	1.09	1.01	1.04
D04	67	16	160	1.34	11.2	9.95	11.42	10.17	11.02	9.22	9.66	9.63	0.87	0.98	0.90	1.08	1.03	1.03
D05	67	16	160	1.34	11.2	10.61	12.21	10.88	11.79	9.87	9.99	10.30	0.87	0.97	0.90	1.08	1.06	1.03
D06	67	16	160	1.34	11.2	11.67	12.66	11.28	12.22	10.23	10.17	12.22	0.92	1.03	0.96	1.14	1.15	0.95
D07	67	16	160	1.34	11.2	11.93	12.83	11.43	12.38	10.36	10.24	12.38	0.93	1.04	0.96	1.15	1.17	0.96
D08	67	16	160	1.34	11.2	12.69	12.98	11.56	12.52	10.48	10.30	12.53	0.98	1.10	1.01	1.21	1.23	1.01
D01	67	16	160	1.34	11.2	13.53	13.07	11.65	12.62	10.56	10.34	12.62	1.03	1.16	1.07	1.28	1.31	1.07
D02	67	16	160	1.34	11.2	14.32	13.71	12.22	13.23	11.08	10.59	13.24	1.04	1.17	1.08	1.29	1.35	1.08
1	67	16	160	1.00	20.83	5.67	7.63	6.80	7.37	6.17	7.90	6.02	0.74	0.83	0.77	0.92	0.72	0.94
2	67	16	160	1.00	20.83	6.85	9.85	8.78	9.52	7.96	8.97	7.78	0.70	0.78	0.72	0.86	0.76	0.88
3	67	16	160	1.00	20.83	7.97	11.66	10.39	11.27	9.42	9.76	9.20	0.68	0.77	0.71	0.85	0.82	0.87
4	67	16	160	1.00	20.83	10.45	13.22	11.78	12.77	10.68	10.40	12.05	0.79	0.89	0.82	0.98	1.01	0.87
5	67	16	160	1.00	20.83	6.97	9.85	8.78	9.52	7.96	8.97	7.78	0.71	0.79	0.73	0.88	0.78	0.90
6	67	16	160	1.00	20.83	8.2	11.66	10.39	11.27	9.42	9.76	9.20	0.70	0.79	0.73	0.87	0.84	0.89
7	42	16	160	1.00	20.83	5.47	5.73	5.55	7.51	4.90	6.32	4.71	0.96	0.99	0.73	1.12	0.86	1.16
8	42	16	160	1.00	20.83	6.37	7.39	7.17	9.69	6.33	7.19	6.08	0.86	0.89	0.66	1.01	0.89	1.05
9	42	16	160	1.00	20.83	6.97	8.75	8.48	11.47	7.49	7.82	7.19	0.80	0.82	0.61	0.93	0.89	0.97
10	42	16	160	1.00	20.83	8.46	9.92	9.62	13.00	8.49	8.32	9.77	0.85	0.88	0.65	1.00	1.02	0.87
11	66	18	180	1.10	20.83	5.1	7.00	6.39	7.42	5.79	7.37	5.61	0.91	0.80	0.69	0.88	0.69	0.91
12	66	18	180	1.10	20.83	6.45	9.03	8.24	9.58	7.48	8.38	7.25	0.89	0.78	0.67	0.86	0.77	0.89
13	66	18	180	1.10	20.83	7.46	10.69	9.76	11.33	8.85	9.11	8.57	0.87	0.76	0.66	0.84	0.82	0.87
14	66	18	180	1.10	20.83	9.95	12.12	11.06	12.85	10.03	9.70	9.72	1.02	0.90	0.77	0.99	1.03	0.88
15	67	16	160	1.00	20.83	6.85	9.85	8.78	9.52	7.96	8.97	7.78	0.70	0.78	0.72	0.86	0.76	0.88
16	67	16	120	1.00	20.83	6.49	10.73	10.10	8.86	7.96	10.18	8.41	0.60	0.64	0.73	0.82	0.64	0.77
17	67	16	80	1.00	20.83	6.22	12.48	12.72	7.53	7.96	12.58	9.67	0.50	0.49	0.83	0.78	0.49	0.64
Mean values													0.81	0.89	0.81	1.00	0.93	0.95
Standard deviation													0.13	0.15	0.14	0.15	0.21	0.11

to the decrease in the bearing which leads to a reduction in bond strength.

4. Analysis of bond stress

4.1. Comparison between the experimental bond strength (τ_u) and other predicted bond strength equations

Several researchers have attempted to formulate equations that represent the bond between the reinforcing bars and the concrete. Below is a brief description of a few: Orangun et al. [1] proposed the following formula:

$$\tau_u = 0.083045\sqrt{\acute{f_c}}\left[1.2 + 3\left(\frac{c}{d_b}\right) + 50\left(\frac{d_b}{L_d}\right)\right] \quad (3)$$

where c is the minimum concrete cover, mm and $\acute{f_c}$ is the cylinder compressive strength of concrete, MPa, d_b is the bar diameter and L_d is the development length.

Darwin et al. [20] proposed a modified expression for bond strength as follows:

$$\tau_u = 0.083045 \times \sqrt{\acute{f_c}}\left[\left(1.06 + 2.12\left(\frac{c}{d_b}\right)\right)\left(0.92 + 0.08\left(\frac{C^*_{max}}{C_{min}}\right) + 75\left(\frac{d_b}{L_d}\right)\right)\right] \quad (4)$$

where $c = min\ (c_x, c_y, c_s/2)$ and $C^*_{max} = max\ (min(c_x, c_s/2), c_y)$ in which c_s is the side cover, c_y is the bottom cover and c_x is the spacing between the bars.

Hadi [22] proposed the following formula of the pullout test for high strength concrete.

$$\tau_u = 0.083045\sqrt{\acute{f_c}}\left[22.8 - 0.208\left(\frac{c}{d_b}\right) - 38.212\left(\frac{d_b}{L_d}\right)\right] \quad (5)$$

Esfahani and Rangan [26] proposed the following formula for high strength concrete with compressive equal to or greater than 50 MPa:

$$\tau_u = 8.6\left(\frac{c/_{d_b+0.5}}{c/_{d_b+5.5}}\right)f_{ct} \quad (6)$$

where c is the minimum cover and f_{ct} is the tensile strength of concrete taken as $0.55\sqrt{\acute{f_c}}$ in MPa.

ACI committee 408 [14] has updated Zuo and Darwin's equation as follows:

$$\frac{T_b}{f_c'^{1/4}} = \frac{T_c + T_s}{f_c'^{1/4}} = \frac{A_b f_s}{f_c'^{1/4}} = [1.43L_d(c_{min} + 0.5d_b) + 57.4A_b]\left(0.1\frac{c_{max}}{c_{min}} + 0.9\right) + \left(8.9t_r t_d\frac{NA_{tr}}{n} + 558\right)f_c'^{1/2} \quad (7)$$

where T_b is the total bond force, which can be represented as the sum of a concrete contribution T_c, representing the bond force that would be developed without the transverse reinforcement, plus a steel contribution T_s, representing the additional bond strength provided by the transverse steel, A_b is the area of steel bar, t_r is the term representing the effect of relative rib area, t_d is the term representing the effect of bar size, n is the number of steel bar, N is the number of transverse stirrups within the development length and A_{tr} is the area of each stirrup.

Based on the measured bond strength for all the specimens and in order to take into account the higher strength of concrete compressive strength, cover, bar diameter, bonded length and the ratio between rib height (h_r) and spacing between ribs (s_r), a new formula is proposed. This proposed equation is drawn as follows:

$$\tau = \sqrt{f_{cu}}\left[0.1377 + 0.1539(c/d_b) + 2.673\left(\frac{d_b}{L_d}\right) + 1.053\left(\frac{h_r}{s_r}\right)\right] \quad \text{for } f_{cu} < 80\text{ MPa} \quad (8)$$

$$\tau = \sqrt{f_{cu}}\left[0.3078 + 0.1539(c/d_b) + 2.673\left(\frac{d_b}{L_d}\right) + 1.053\left(\frac{h_r}{s_r}\right)\right] \quad \text{for } f_{cu} < 80\text{ MPa} \quad (9)$$

where τ_u is the ultimate tensile bond strength in MPa, f_{cu} is the cube compressive strength in MPa, h_r is rib height and s_r is the spacing between ribs.

The experimental test results of ultimate bond strength and the predicted ultimate bond strength obtained using equations of Orangun et al. [1], Drawin et al. [20], Hadi [22], Esfahani and Rangan [26], ACI committee 408 [14] and proposed equation are presented in Tables 6 and 7. Comparing with the previous mention predicted equations and proposed equation, as illustrated in Fig. 14 and Tables 6 and 7; proposed equation provides a better match with the test results. A mean ratio of test results to proposed equation results is 1.01, 1.00 and 0.95 with standard deviation (SD) of 0.05, 0.07and 0.11, for pink lime stone, gravel and dolomite concrete, respectively.

The ultimate pull-out bond test results in this study are less than those obtained using Orangun's et al., Muhammad Hadi's and ACI equations, where the mean ratio of experimental test results to values obtained predicted equations of the previous researchers is 0.85, 0.88 and 0.87 for pink lime stone concrete with SD of 0.04, 0.05 and 0.07, respectively. These ratios for gravel concrete are 0.84, 0.87 and 0.80 with standard division of 0.06, 0.07 and 0.10, respectively, while these ratios for dolomite concrete are 0.81, 0.81 and 0.93 with SD of 0.13, 0.14 and 0.21, respectively, so these previous equations give overestimate bond strength. However, Drawin's et al. and Esfahani and Rangan's equations give good results, where these ratios for pink lime stone concrete are 0.95 and 1.05 with SD of 0.05 and 0.06, while for gravel concrete these ratios are 0.95 and 1.04 with SD of 0.07 and 0.08, respectively. In addition, these ratios for dolomite concrete are 0.89 and 1.00 with SD of 0.15 and 0.15, respectively. Generally, Darwin's et al. and Esfahani and Rangan's predicted equation achieve the best ratios between test results and values predicted using these equations compared with those obtained using Orangun's et al., Muhammad Hadi's and ACI equations.

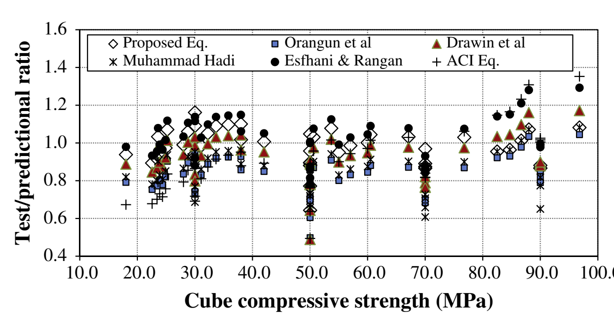

Figure 14 Experimental bond strength test results-prediction ratios versus cube compressive strength for concrete containing different type of coarse aggregate.

To evaluate proposed equation, another comparison was made using test data of Idun and Darwin [27], where the ASTM A 944 test beam developed by Darwin and Graham [28], was used and each specimen contained a 25 mm nominal diameter bottom-cast test bar with 51 mm cover and 381 mm of concrete above the bar. By using these data (14 specimens), the mean ratio between test results of Emmanuel study and Orangun's et al., Drawin's et al. and proposed equation is 0.82, 0.83 and 0.87 with SD of 0.03, 0.03 and 0.04, respectively. So, the result of proposed equation matches with Orangun's et al. and Drawn's et al. equation result. Proposed equation Eqs. (8) and (9) can predict the bond strength accurately.

4.2. A new trend of proof bond strength

Figs. 5–8 show the relationship between the bond stress and slip, and it is observed that this relation is divided into two stages up to the ultimate strength. At the first stage, the friction is responsible for transferring the tensile stresses to the concrete. This stage shows almost a constant rate of increasing in the slip with the corresponding stress increase till a certain point (point of deviation). After that point, the second stage takes place where there is a change in the slope of the relation. At this stage, the bearing is the responsible for transferring the stresses to the concrete. The point of deviation is called the friction bond limit (τ_f) after which the friction is significantly reduced. The results of the points of deviation are collected as shown in Table 8. From this table, it is clear that the ratio between the friction bond strength and the ultimate bond strength (τ_f/τ_u) has an approximate range of 55–78%.

4.3. Proposed idealized bond stress–slip relationship

Fig. 15 shows the proposed idealized bond stress–slip relationship, where point (a) represents the friction bond limit (τ_f), and point (d) represents the ultimate bond strength (τ_u). It was observed that the presence of fully cracked specimen led to a loss in the ultimate bond strength of about 30%. The average ratio of τ_f/τ_u for tested specimen is about 68% while the obtained minimum value of this ratio is 55%, so the proposed ratio of τ_f/τ_{um} is taken as follows

$$\frac{\tau_f}{\tau_u} = \overline{R}u - 2.3(\sigma) = 52.0\% \approx 50\% \tag{10}$$

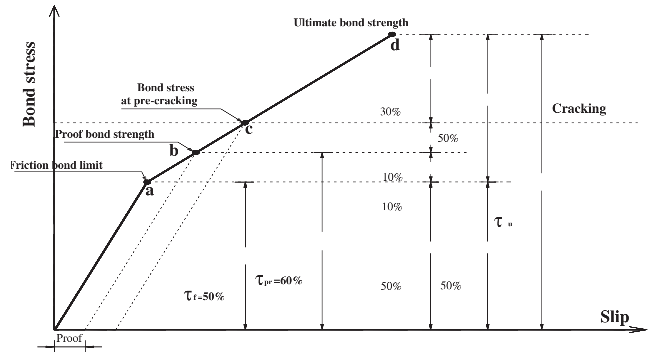

Figure 15 Proposed idealized bond stress–slip relationship.

To obtain the design ultimate bond strength, proof bond strength (τ_{pr}) is suggested. For deformed bar, all tested specimen was split at the end of the test, thus proof bond strength (τ_{pr}) is proposed to be equal to the friction bond strength (τ_f) plus 50% of the bearing bond strength before cracking. This means that the proof bond strength can be taken 60% of the ultimate bond strength as shown in Fig. 15.

4.4. Proposed equations to calculate the design ultimate bond stress and the required development length

The following equation was derived to calculate the ultimate bond stress, proof bond strength (τ_{pr}),

$$\tau_{pr} = \sqrt{f_{cu}}\left[0.08262 + 0.09234(c/d_b) + 1.6038\left(\frac{d_b}{L_d}\right) + 0.6318\left(\frac{h_r}{s_r}\right)\right]$$
$$\text{for } f_{cu} < 80\,\text{MPa} \tag{11}$$

Table 8 Ratio of friction bond limit to ultimate bond strength (τ_f/τ_u).

Spec	C (mm)	d_b (mm)	L_d (mm)	τ_u (MPa)	τ_f (MPa)	τ_f/τ_u (%)
1	67	16	160	5.67	3.73	66
2	67	16	160	6.85	4.98	73
3	67	16	160	7.97	5.47	69
4	67	16	160	10.45	6.47	62
5	67	16	160	6.97	4.00	57
6	67	16	160	8.20	4.50	55
7	42	16	160	5.47	3.50	64
8	42	16	160	6.37	4.50	71
9	42	16	160	6.97	5.5	78
10	42	16	160	8.46	6.00	71
11	67	18	180	5.10	3.98	78
12	67	18	180	6.45	4.98	77
13	67	18	180	7.46	5.00	67
14	67	18	180	9.95	5.97	60
15	67	16	160	6.85	4.98	73
16	67	16	120	6.494	4.35	66
17	67	16	80	6.22	4.30	69
Mean values ($\overline{Ru}$)						68.05
Standard deviation (σ)						6.96

Table 9 Comparison between design ultimate bond stress of proposed equation and those calculated using BS and EN equations.

Type of coarse agg.	Mix no.	Design ultimate bond stress (MPa)			Proposed values/prediction values according to BS & EN ratios		Type of coarse agg	Mix no.	Design ultimate bond stress (MPa)			Proposed values / Prediction values according to BS & EN ratios	
		Proposed Eqs. (11) and (12) (a)	BS Eq. (13) (1)	EN Eq. (14) (2)	(a)/(1)	(a)/(2)			Proposed Eqs. (11) and (12) (a)	BS Eq. (1)	EN Eq. (2)	(a)/(1)	(a)/(2)
Pink lime stone	L01	2.32	1.97	2.28	1.18	1.02	Dolomite	D01	3.34	2.85	3.84	1.18	0.87
	L02	2.28	1.94	2.24	1.18	1.02		D02	3.44	2.93	3.98	1.18	0.86
	L03	2.36	2.01	2.34	1.18	1.01		D03	3.66	3.11	4.31	1.18	0.85
	L04	2.52	2.15	2.55	1.18	0.99		D04	3.85	3.28	4.56	1.18	0.84
	L05	2.58	2.19	2.62	1.18	0.98		D05	4.12	3.50	4.60	1.18	0.90
	L06	2.90	2.47	3.07	1.18	0.94		D06	4.89	3.63	4.79	1.35	1.02
	L07	3.05	2.59	3.28	1.18	0.93		D07	4.95	3.68	4.84	1.35	1.02
	L08	3.32	2.83	3.69	1.18	0.90		D08	5.01	3.72	4.89	1.35	1.02
	L09	3.49	2.97	3.99	1.18	0.87		D09	5.05	3.75	4.92	1.35	1.03
	L10	3.55	3.02	4.05	1.18	0.88		D10	5.30	3.94	5.15	1.35	1.03
	L11	3.64	3.10	4.28	1.18	0.85		1	2.41	2.19	2.70	1.10	0.89
	Mean values				1.18	0.94		2	3.11	2.83	3.74	1.10	0.83
	Standard deviation				0.00	0.06		3	3.68	3.35	4.66	1.10	0.79
Gravel	G01	2.00	1.70	1.87	1.18	1.07		4	4.82	3.79	4.96	1.27	0.97
	G02	2.23	1.90	2.17	1.18	1.03		5	3.11	2.83	3.74	1.10	0.83
	G03	2.28	1.94	2.22	1.18	1.02		6	3.68	3.35	4.66	1.10	0.79
	G04	2.30	1.95	2.25	1.18	1.02		7	1.88	2.19	2.70	0.86	0.70
	G05	2.35	2.00	2.32	1.18	1.01		8	2.43	2.83	3.74	0.86	0.65
	G06	2.49	2.12	2.51	1.18	0.99		9	2.88	3.35	4.66	0.86	0.62
	G07	2.62	2.23	2.69	1.18	0.98		10	3.91	3.79	4.96	1.03	0.79
	G08	2.67	2.27	2.75	1.18	0.97		11	2.25	2.19	2.70	1.02	0.83
	G09	2.73	2.32	2.83	1.18	0.96		12	2.90	2.83	3.74	1.02	0.78
	G10	2.81	2.39	2.95	1.18	0.95		13	3.43	3.35	4.66	1.02	0.74
	G11	2.90	2.47	3.07	1.18	0.94		14	4.53	3.79	4.96	1.20	0.91
	Mean values				1.18	1.00		15	3.11	2.83	3.74	1.10	0.83
	Standard deviation				0.00	0.04		16	3.36	2.83	3.74	1.19	0.90
								17	3.87	2.83	3.74	1.37	1.03
								Mean values				1.14	0.86
								Standard deviation				0.15	0.12

Table 10 Comparison between required development length of proposed equation and those calculated using BS and ACI 318 equations.

Type of coarse agg.	Mix no.	Development length (mm)			Ratio of proposed values/prediction values according to BS & ACI		Type of coarse agg	Mix no.	Development length (mm)			Ratio of proposed values/prediction values according to BS & ACI	
		Proposed Eqs. (11) and (12) (a)	BS Eq. (13) (1)	ACI 318 Eq. (17) (2)	(a)/(1)	(a)/(2)			Proposed Eqs. (11) and (12) (a)	BS Eq. (13) (1)	ACI 318 Eq. (17) (2)	(a)/(1)	(a)/(2)
Pink lime stone	L01	620.5	729.4	621.3	0.85	1.00	Dolomite	D01	430.5	506.1	420.7	0.85	1.02
	L02	630.6	741.2	631.4	0.85	1.00		D02	418.0	491.4	409.3	0.85	1.02
	L03	610.1	717.1	610.9	0.85	1.00		D03	393.7	462.8	386.0	0.85	1.02
	L04	570.7	670.8	571.4	0.85	1.00		D04	373.9	439.5	369.8	0.85	1.01
	L05	559.2	657.3	559.9	0.85	1.00		D05	349.5	410.8	351.2	0.85	1.00
	L06	496.8	584.0	497.5	0.85	1.00		D06	294.6	396.3	332.6	0.74	0.89
	L07	472.6	555.5	473.2	0.85	1.00		D07	290.7	391.2	327.8	0.74	0.89
	L08	433.1	509.1	433.7	0.85	1.00		D08	287.4	386.7	323.2	0.74	0.89
	L09	413.0	485.4	408.9	0.85	1.01		D09	285.2	383.8	321.0	0.74	0.89
	L10	405.7	476.8	404.4	0.85	1.00		D10	271.9	365.9	301.1	0.74	0.90
	L11	395.4	464.8	387.9	0.85	1.02		1	597.51	657.26	548.6	0.91	1.09
	Mean values				0.85	1.00		2	462.83	509.11	429.4	0.91	1.08
	Standard deviation				0.00	0.01		3	391.16	430.28	364.3	0.91	1.07
Gravel	G01	721.6	848.2	722.6	0.85	1.00		4	298.77	379.47	316.7	0.79	0.94
	G02	644.8	757.9	645.6	0.85	1.00		5	462.83	509.11	429.4	0.91	1.08
	G03	632.9	744.0	633.7	0.85	1.00		6	391.16	430.28	364.3	0.91	1.07
	G04	626.9	736.9	627.7	0.85	1.00		7	764.67	657.26	548.6	1.16	1.39
	G05	613.8	721.4	614.6	0.85	1.00		8	592.31	509.11	429.4	1.16	1.38
	G06	578.8	680.3	579.5	0.85	1.00		9	500.59	430.28	364.3	1.16	1.37
	G07	549.4	645.8	550.1	0.85	1.00		10	368.55	379.47	316.7	0.97	1.16
	G08	539.4	634.0	540.1	0.85	1.00		11	641.29	657.26	617.1	0.98	1.17
	G09	527.9	620.5	528.6	0.85	1.00		12	496.74	509.11	483.1	0.98	1.16
	G10	511.9	601.7	512.5	0.85	1.00		13	419.82	430.28	409.8	0.98	1.15
	G11	497.0	584.1	497.6	0.85	1.00		14	317.55	379.47	356.3	0.84	1.00
	Mean values				0.85	1.00		15	462.83	509.11	429.4	0.91	1.08
	Standard deviation				0.00	0.00		16	428.15	509.11	429.4	0.84	1.00
								17	372.35	509.11	429.4	0.73	0.87
								Mean values				0.89	1.06
								Standard deviation				0.13	0.15

$$\tau_{pr} = \sqrt{f_{cu}}\left[0.18468 + 0.09234(c/d_b) + 1.6038\left(\frac{d_b}{L_d}\right) + 0.6318\left(\frac{h_r}{s_r}\right)\right]$$
$$\text{for } f_{cu} \geqslant 80\,\text{MPa} \quad (12)$$

The results calculated using the previous two equations (Eq. 11 and 12) are divided by 1.5 factor of safety to assess the design ultimate bond stress.

The design ultimate bond stress to BS 8110 [29] and EN [30] is calculated using Eqs. (13) and (14).

$$f_{bu} = 0.4\sqrt{f_{cu}} \quad \text{for BS} \quad (13)$$

where f_{bu} is the design ultimate bond stress.

$$f_{bu} = 2.25\eta_1\ \eta_2 f_{ctd} \quad \text{for EN} \quad (14)$$

where η_1 is a coefficient related to the quality of the bond condition and the position, η_2 is related to the bar equals to 1.0 for bar diameter $\leqslant$32 mm and f_{ctd} is the design value of concrete tensile strength calculated using Eqs. (15) or (16) according to EN [30].

$$f_{ctd} = (0.21 f_{cu}^{\frac{2}{3}})/\gamma c \quad \text{for } f_{cu} \leqslant 60\ \text{MPa} \quad (15)$$

$$f_{ctd} = 1.484 ln(1 + (f_{cu} + 8)/10)/\gamma c \quad \text{for } f_{cu} > 60\ \text{MPa} \quad (16)$$

Where $\gamma_c = 1.5$

Table 9 shows the design ultimate bond stress of the tested specimens using Eqs. (11)–(14). Comparing with the design ultimate bond stress determined using these equations, proposed equation provides a better match with EN results. A mean ratio between design ultimate bond stress determined using proposed equation and BS equation is 1.18, 1.18 and1.14 with SD of 0.0, 0.0 and 0.15 for pink lime stone, gravel, dolomite concrete, respectively, while this ratio for EN are 0.94, 1.0 and 0.86 with SD of 0.06, 0.04 and 0.12, respectively. Values of design ultimate bond stresses obtained using proposed equation agree well with the values determined using BS and EN equations.

To calculate the required development length, proposed Eqs. (11) and (12) and BS equation (Eq. (13)) have been used. ACI 318 [17] is used to calculate the required development length using the following equation:

$$L_d = \left(\frac{f_y \psi_t \psi_e}{2.1\lambda\sqrt{\acute{f_c}}}\right) d_b \quad (17)$$

where ψ_t is the traditional reinforcement location factor, ψ_e is a coating factor λ is based on the concrete type, for normal weight concrete, it equals to 1.0.

Also the yield strength of steel used to calculate development length is 360 MPa. Table 10 shows the required development length results calculated using proposed, BS and ACI 318 equations [18]. From this table, proposed equation provides a better match with the results obtained using ACI 318 equation, where the ratio between development lengths using the proposed equations to that using ACI 318 equation, where the ratio between development lengths using the proposed equations to that using ACI equation almost equals to 1.0. The development length of proposed equation is less than that of BS by 17.6% for pink lime stone and gravel concrete and by 12% for dolomite concrete.

5. Conclusions

Based on the experimental test results, the following conclusions can be drawn:

1. For a concrete with the same compressive strength, the tensile pull-out bond strength is lower than the single pull-out bond strength. The pull-out bond strength of crushed dolomite and crushed pink lime stone concrete is higher than that of gravel concrete.
2. The characteristic ratio of ultimate tensile pull-out bond strength and pull-out bond strength is 0.82, 0.86 and 0.81 for crushed pink lime stone, gravel or crushed dolomite concrete, respectively, so, one can perform such a simple pull-out test and multiply the strength by the previous ratios.
3. High strength concrete specimens fail in a brittle manner, and the specimens fail abruptly forming longitudinal splitting cracks.
4. As the pre-crack length increases, the bond tensile strength decreases and the corresponding slip increases. The fully cracked specimen losses 30% of the ultimate bond strength of un-cracked section bond strength.
5. Proof bond strength is proposed to represent the bond stress used in ultimate design. Equations to calculate ultimate design bond stress are proposed. There is a good agreement between results of these equations and those of EN equation. The development length calculated using the proposed equations represent 0.86 and 1.02 that given by BS and ACI 318 equations, respectively.

References

[1] C.O. Orangun, I.O. Jirsa, J.E. Breen, A re-evaluation of test data on development length and splices, ACI J. 74 (3) (1977) 114–122.
[2] A. Al-Negheimish, R.Z. Al-Zaid, Effect of manufacturing process and rusting on the bond behavior of deformed bars in concrete, Cem. Concr. Compos. 26 (6) (2004) 735–742.
[3] K. Ahmed, Z.A. Siddiqi, M. Ashraf, A. Ghaffar, Effect of rebar cover and development length on bond and slip in high strength concrete, Pakistan J. Eng. Appl. Sci. 2 (2008).
[4] P. Robert, P. Thomas, Reinforced Concrete Structures, John Wiley & Sons, New York, 1975.
[5] Yuxi Zhao, Hongwei Lin, Wu Kang, Weiliang Jin, Bond behaviour of normal/recycled concrete and corroded steel bars, Constr. Build. Mater. 48 (2013) 348–359.
[6] RILEM, Essai portant sur l'adhérence des armatures de béton – Essai par traction, Matér. Constr. 3 (15) (1970) 175–178.
[7] R.P. Tastani, S.J. Pantazopulou, Experimental evaluation of the direct tension-pullout bond test. Bond in concrete – from research to standards, Budapest, 2002.
[8] B.S. Hamad, Bond strength improvement of reinforcing bars with specially designed rib geometries, ACI Struct. J. 92 (1) (1995) 3–13.
[9] A. Castel, T. Vidal, K. Viriyametanont, R. François, Effect of reinforcing bar orientation and location on bond with self-consolidating concrete, ACI Struct. J. 103 (4) (2006) 559–567.
[10] C. La Borderie, G. Pijaudier-Cabot, Influence of the state of stress in concrete on the behavior of the steel concrete interface, in: Concrete fracture mechanics of structures, Colorado, USA, 1992.
[11] L.J. Malvar, Bond of reinforcement under controlled confinement, ACI Mater. J. 89 (6) (1992) 593–601.
[12] A. Torre-Casanova, L. Jason, L. Davenned, X. Pinelli, Confinement effects on the steel–concrete bond strength and pull-out failure, Eng. Fract. Mech. 97 (2013) 92–104.

[13] J.A. Joseph, A.I. Camille, Bond strength of epoxy-coated bars in underwater concrete, Constr. Build. Mater. 30 (2012) 667–674.
[14] ACI Committee 408R-03, Bond and Development of Straight Reinforcing Bars in Tension, American Concrete Institute, Farmington Hills, Mich., 2003, 1.111.
[15] L. De Anda, C. Courtier, J. Moehle, Bond strength of prefabricated epoxy-coated reinforcement, ACI Struct. J. 103 (2) (2006) 226–234.
[16] O.C. Choi, H. Hadje-Ghaffari, D. Darwin, S.L. McCabe, Bond of epoxy-coated reinforcement: bar parameter, ACI Mater. J. (2) (1991) 207–217.
[17] ACI Committee 318-08, Building Code Requirements for Reinforced Concrete, American Concrete Institute, Farmington Hills, Mich., 2008.
[18] AASHTO, Standard Specification for Highway Bridges, 14th ed., American Association of State Highway and Transportation Officials, Washington (DC), 1989.
[19] Zsutty, Empirical study for bar development behavior, J. Struct. Eng. ASCE 111 (1) (1985) 205–219.
[20] Darwin, S.L. Maccab, E.K. Indun, S.P. Scheonekase, Development length criteria; bars not confined by transverse reinforcement, ACI J. 89 (6) (1992) 709–720.
[21] J. Zuo, D. Darwin, Splice strength of conventional and high relative rib area bars in normal and high strength concrete, ACI Struct. J. 97 (4) (2000) 630–641.
[22] Muhammad N.S. Hadi, Bond of high strength concrete with high strength reinforcing steel, Open Civ. Eng. J. (2008) 2143–2147.
[23] Kazim Turk, Bond strength of reinforcement in splices in beams. Structural Engineering and Mechanics No. 4, 2003.
[24] M. Alavi-Fard, H. Marzouk, Bond of high strength concrete under monotonic pullout loading, Mag. Concr. Res. 56 (9) (2004) 545–557.
[25] K. Ahmed, Z.A. Siddiqi, M. Yousaf, Slippage of steel in high and normal strength concrete, Pakistan J. Eng. Appl. Sci. 1 (2007) 31–40.
[26] M.R. Esfahani, B.V. Rangan, Bond between normal strength and high-strength concrete (HSC) and reinforcing bars in splices in beams, ACI Struct. J. 95 (3) (1998) 272–280.
[27] Emmanuel K. Idun, David Darwin, Bond of epoxy-coated reinforcement: coefficient of friction and rib face angle, ACI Struct. J. 96 (4) (1999) 609–616.
[28] D. Darwin, E.K. Graham, Effect of Deformation Height and Spacing on Bond Strength of Reinforcing Bars, ACI Struct. J. 90 (6) (1993) 646–657.
[29] BS 8110-1: 1997, Part 1: Code of Practice for Design and Construction, 2002, pp. 89–90.
[30] EN 1992-1-1, Eurocode 2: Design of Concrete Structures – Part 1-1: General Rules and Rules for Buildings, 2004.